DALTON
FULL PAPER

A very short Re_2^{6+} quadruple bond: first DFT calculations on a paddlewheel complex with an element of the third transition series

F. Albert Cotton,*[a] Jiande Gu,[a] Carlos A. Murillo*[a,b] and Daren J. Timmons[a]

[a] *Laboratory for Molecular Structure and Bonding and Department of Chemistry, Texas A&M University, College Station, TX 77843-3255, USA*
[b] *Department of Chemistry, University of Costa Rica, Ciudad Universitaria, Costa Rica*

Received 11th June 1999, Accepted 12th August 1999

The first complexes containing third row transition elements with bridging hpp (the anion of 1,3,4,6,7,8-hexahydro-2*H*-pyrimido[1,2-*a*]pyrimidine) are presented. $Re_2(hpp)_4Cl_2$, **1**, is a typical paddlewheel complex with two axial chloride ions. The Re–Re distance in **1** of 2.191(1) Å is one of the shortest known for a quadruply-bonded Re_2^{6+} complex and the Re–Cl distance of 2.749(5) Å is the longest one reported for this type of complex. The second compound, $Re_2(hpp)_3Cl_3$, **2**, has three bridging hpp ligands, two equatorial chloride ions and one axial chloride ion. The Re–Re distance is 2.189(2) Å. The electronic structure of **1** has been determined by DFT calculations, the first time this has been done on a paddlewheel complex containing a third row transition element.

Introduction

As explained elsewhere,[1] we began several years ago to use the hpp ligand, I (the anion of 1,3,4,6,7,8-hexahydro-2*H*-

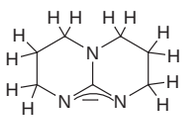

I

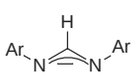

II

pyrimido[1,2-*a*]pyrimidine), mainly because we sought a ligand that would be similar to the DArF ligand, II (*N*′,*N*′-diarylformamidinate), but have greater resistance to chemical attack leading to decomposition. We have since discovered that while hpp fulfilled our initial requirement, allowing, for example, the preparation of the first compound with an Nb_2^{4+} core,[2a] it has other advantages over DArF ligands. It has enabled the preparation of $[Mo_2(hpp)_4][BF_4]_2$[2b] and $Pd_2(hpp)_4Cl_2$[2c] neither of which has any DArF analogue, as well as several other compounds that do have DArF analogues.[2d,e] Clearly, there are some significant stereoelectronic differences between hpp and the DArF ligands, in addition to the superior stability of the former.

Heretofore, no M_2^{n+} complex with the hpp ligand has been reported with a metal from the third transition series. We have now made such complexes for all of the metals from W to Pt, and we describe here the results obtained with rhenium. These, as will be seen, emphasize that hpp is no mere stand-in for DArF but rather, it can produce compounds that display important differences from their DArF analogues.

In the case of $Re_2(hpp)_4Cl_2$ we find quite different Re–Re and Re–Cl distances from those in $Re_2(DTolF)_4Cl_2$ (DTolF = *N*,*N*′-di-*p*-tolylformamidinate) which was reported several years ago.[3] These surprising differences motivated theoretical studies that are also presented here. These theoretical studies occupy a prominent place in this report because they are the first of many similar ones that will be discussed in future papers.

Experimental

The starting materials, $[NBu_4]_2Re_2Cl_8$ and Hhpp were purchased from Aldrich; Hhpp was purified by sublimation prior to use. Solvents were freshly distilled under N_2 from suitable drying agents. All manipulations were carried out under a nitrogen atmosphere using standard Schlenk-line techniques unless otherwise stated. The IR spectrum was recorded on a Perkin-Elmer 16PC FT-IR spectrophotometer as a KBr pellet. The UV-vis spectrum was recorded on a Cary-17D spectrometer. The ^1H NMR spectrum was collected on a Varian 200 spectrometer. FAB mass spectrum measurements were acquired on a VG Analytical 70S (Manchester, UK) high resolution, double-focusing, magnetic-sector mass spectrometer.

Preparations

$Re_2(hpp)_4Cl_2$, 1. (A) Lihpp (1.0 mmole) was prepared *in situ* from Hhpp and MeLi in 5 ml THF, and then added *via* cannula to a solution of $[NBu_4]_2Re_2Cl_8$ (0.25 g, 0.22 mmole) in 10 ml of acetonitrile. The blue-green solution quickly turned deep green; it was refluxed overnight. A bright purple solid precipitated and the solution became yellow-brown. The solid, **1**, was collected on a frit and washed with 3 × 8 ml acetone. Yield: 64% (0.14 g, 0.14 mmole). (B) A Schlenk tube was charged with $[Bu_4N]_2Re_2Cl_8$ (0.25 g, 0.22 mmole), Hhpp (0.55 g, 4.0 mmole) and a small stir bar. The mixture was heated at 145 °C for 6 h while stirring; it afforded a purple residue. After the residue cooled to room temperature, it was washed with THF and acetonitrile to remove excess Hhpp and any unreacted $[Bu_4N]_2Re_2Cl_8$. The undissolved bright purple powder, **1**, was washed with diethyl ether and dried under vacuum. Yield: 55% (0.12 g, 0.12 mmole). The complex is stable in air as a solid and in solution. Crystals suitable for X-ray diffraction were grown by the slow diffusion of a layer of hexanes into a dichloromethane solution of **1**. ^1H NMR ($CDCl_3$): δ 3.74 (t, CH_2), 3.48 (t, CH_2), 1.89 (quin, CH_2). IR (KBr, cm^{-1}): 2927.0 (m), 2852.8 (m), 1637.3 (w), 1535.3 (vs), 1491.6 (s), 1471.9 (m), 1448.4 (s), 1390.6 (m), 1311.0 (s), 1279.1 (m), 1261.7 (m), 1216.0 (s), 1135.7 (m), 1069.8 (m), 1050.3 (m), 802.3 (m), 752.9 (m), 712.0 (w). UV-vis ($CHCl_3$, nm): 725 (sh), 650, 360, 285. FAB(+)MS: *m*/*z* 959 $[M - Cl]^+$.

$Re_2(hpp)_3Cl_3$, 2. Lihpp (1.0 mmole) was prepared *in situ* in 5 ml THF and added to a suspension of $[NBu_4]_2Re_2Cl_8$ (0.25 g,

Table 1 Crystallographic parameters for $Re_2(hpp)_4Cl_2$, **1**, and $Re_2(hpp)_3Cl_3$, **2**·$(CH_3)_2CO$

	1	**2**·$(CH_3)_2CO$
Formula	$C_{28}H_{48}Cl_2N_{12}Re_2$	$C_{24}H_{42}Cl_3N_9Re_2$
M	996.08	951.42
Lattice symmetry	Tetragonal	Monoclinic
Space group	$I4/m$	$I2/a$
a/Å	10.0040(8)	24.985(8)
b/Å	10.0040(8)	10.17(2)
c/Å	15.871(2)	23.984(8)
β/°		90.02(1)
V/Å^3	1588.4(3)	6093(10)
Z	2	8
d_{calc}/g cm^{-3}	2.083	2.075
μ/mm^{-1}	7.825	8.239
Radiation (λ/Å)	Mo-Kα (0.71073)	
T/K	213	
Residuals: $R1$, $wR2$	0.041, 0.095	0.052, 0.126
Weight parameters	0.0, 29.15	0.036, 314.27
Largest peak/e Å^{-3}	1.9(2)	2.3(2)

Table 2 Selected bond lengths (Å) and angles (°) for $Re_2(hpp)_4Cl_2$, **1**

Re(1)–Re(1)#1	2.1913(12)
Re(1)–N(11)	2.070(7)
Re(1)–Cl(1)	2.749(5)
N(11)–Re(1)–N(11)#2	177.2(3)
N(11)–Re(1)–N(11)#3	89.967(8)
N(11)–C(17)–N(11)#4	117.0(10)

Symmetry transformations used to generate equivalent atoms: #1 $-x$, $-y$, $-z$; #2 $-x$, $-y$, z; #3 y, $-x$, z; #4 x, y, $-z$.

Table 3 Selected bond lengths (Å) and angles (°) for $Re_2(hpp)_3Cl_3$, **2**·$(CH_3)_2CO$

Re(1)–Re(2)	2.189(2)
Re(1)–N(11)	2.089(12)
Re(1)–N(21)	2.098(11)
Re(1)–N(31)	2.107(10)
Re(1)–Cl(1)	2.407(4)
Re(1)–Cl(3)	2.597(4)
Re(2)–N(32)	2.004(11)
Re(2)–N(22)	2.011(12)
Re(2)–N(12)	2.042(13)
Re(2)–Cl(2)	2.372(4)
N(11)–Re(1)–N(21)	178.3(4)
N(11)–Re(1)–N(31)	91.3(5)
N(21)–Re(1)–N(31)	90.5(4)
N(11)–Re(1)–Cl(1)	87.9(3)
N(21)–Re(1)–Cl(1)	90.3(3)
N(31)–Re(1)–Cl(1)	171.2(3)
Re(2)–Re(1)–Cl(1)	99.6(1)
N(11)–Re(1)–Cl(3)	89.7(3)
N(21)–Re(1)–Cl(3)	90.0(3)
N(31)–Re(1)–Cl(3)	87.7(3)
Re(2)–Re(1)–Cl(3)	176.85(9)
Cl(1)–Re(1)–Cl(3)	83.5(2)
N(32)–Re(2)–N(22)	90.7(5)
N(32)–Re(2)–N(12)	91.6(5)
N(22)–Re(2)–N(12)	174.0(4)
N(32)–Re(2)–Cl(2)	149.5(3)
N(22)–Re(2)–Cl(2)	87.0(3)
N(12)–Re(2)–Cl(2)	88.2(3)
Re(1)–Re(2)–Cl(2)	117.3(1)
N(12)–C(17)–N(11)	117(1)
N(22)–C(27)–N(21)	116(1)
N(32)–C(37)–N(31)	118(1)

0.22 mmole) in 10 ml THF and refluxed overnight. A mixture of purple and green solids precipitated. The purple solid was **1**. The green solid was extracted from the mixture with acetone. The extract was concentrated to green crystals of **2**·$(CH_3)_2CO$. The yield was not established for this complex.

X-Ray crystallography

In each case, the data were collected on a Nonius FAST area-detector system. Typical procedures for our laboratory have been previously described.[2d] Complex **1** was refined in space group $I4/m$. The molecule sits on a special position and the metal–metal bond is along the 4-fold axis. Because of static disorder, the ligands were modeled in two positions each of occupancy *ca.* 50%. Complex **2**·$(CH_3)_2CO$ was refined in space group $I2/a$; some portions of the ligands in this structure were also modeled in two positions; ligand disorder is not uncommon in $M_2(hpp)_4Cl_2$ compounds.[1] The 2/m axial symmetry was confirmed with axial photographs. Data were corrected for absorption using a multi-scan procedure. Because of the high absorption coefficients of the crystals, not all spurious peaks could be fully corrected. All non-disordered, non-hydrogen atoms were refined with anisotropic displacement parameters. All hydrogen atoms were placed in calculated positions and refined constrained to their parent atoms. Both structures refined well giving acceptable figures of merit. Crystallographic parameters are summarized in Table 1 and selected bond distances and angles are shown in Table 2 for **1** and in Table 3 for **2**.

CCDC reference number 186/1622.

Discussion

Experimental results

The reaction of Hhpp or Lihpp with third row transition elements through established methods gives the expected rhenium paddlewheel complexes. While several complexes containing an Re_2^{6+} core exist, there are only a handful that employ bridging ligands other than carboxylates.[4]

The melt reaction of $[NBu_4]_2Re_2Cl_8$ with a ligand, a generally useful, established method for the preparation of this type of complex, again proved its usefulness:

$$[NBu_4]_2Re_2Cl_8 + 8Hhpp \xrightarrow{145\ ^\circ C} Re_2(hpp)_4Cl_2 + 4H_2hppCl + 2NBu_4Cl$$

When the reaction of the rhenium starting material with Lihpp is conducted in an acetonitrile–THF mixture (2:1), the synthesis of $Re_2(hpp)_4Cl_2$ is straightforward. The reaction proceeds cleanly under reflux, depositing the product in >60% yield:

$$[NBu_4]_2Re_2Cl_8 + 4Lihpp \xrightarrow[\text{reflux}]{CH_3CN\text{–}THF} Re_2(hpp)_4Cl_2 + 4LiCl + 2NBu_4Cl$$

However, when conducted in refluxing THF, the reaction yielded a mixture of $Re_2(hpp)_4Cl_2$ and the incomplete substitution product, $Re_2(hpp)_3Cl_3$. Compound **2** can also be isolated from the melt when the reaction time is short.

The structure of **1**, a dirhenium unit bridged by four hpp ligands with loosely bound chloride ions in the axial positions, is shown in Fig. 1. Methylene groups of the hpp ligands are disordered over two positions.

The Re–Re bond distance of 2.191(1) Å in **1** is one of the shortest of any Re_2^{6+} complex (the shortest for a tetrabridged complex) and the Re–Cl bond distance of 2.749(5) Å is the longest reported (by *ca.* 0.1 Å). The metal–metal distance is *ca.* 0.09 Å shorter than that in $Re_2(DTolF)_4Cl_2$ (2.2759(3) Å)[3] (DTolF = *N*,*N*′-di-*p*-tolylformamidinate) and slightly shorter than those in $Re_2(L^1)_4Cl_2$ (2.208(2) Å) (L^1 = dimethylbenzamidinato),[5] $Re_2(L^2)_4Cl_2$ (2.206(2) Å) (L^2 = hydroxypyridinato)[6] and the $Re_2(O_2CR)_4Cl_2$ complexes (2.20–2.24Å).[4]

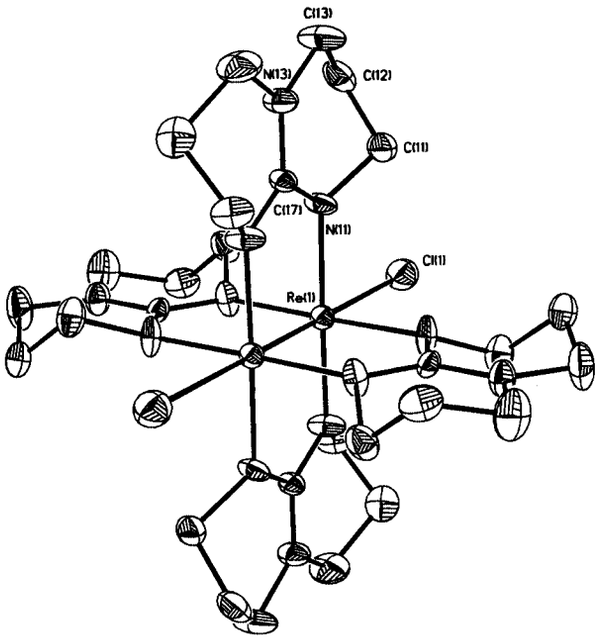

Fig. 1 Molecular structure of $Re_2(hpp)_4Cl_2$, **1**, with ellipsoids at the 50% probability level. Hydrogen atoms and disorder have been omitted for clarity.

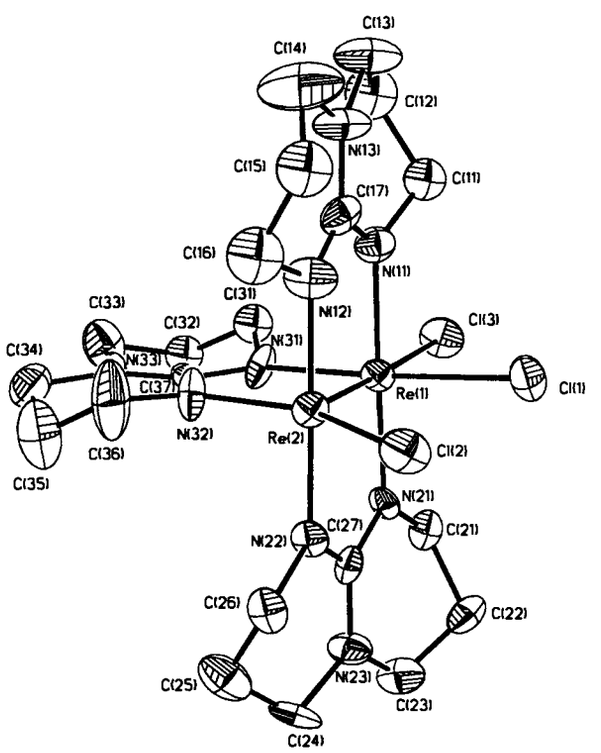

Fig. 2 Molecular structure of $Re_2(hpp)_3Cl_3$, **2**·$(CH_3)_2CO$, with ellipsoids at the 50% probability level. Hydrogen atoms and disorder have been omitted for clarity.

The structure of **2** (Fig. 2) shows an incomplete paddlewheel-type motif containing an Re_2^{6+} core surrounded by three bridging hpp ligands, two equatorial chlorine atoms and one axial chlorine atom. The Re–Re bond distance in **2** of 2.189(2) Å, essentially identical to that in **1**, is also remarkably short. While the axial position on Re(2) is open (not coordinated to either an adjacent molecule (as seen in $Re_2(OMe)_3Cl_3$)[7] or an interstitial acetone molecule), Cl(2) is not strictly in an equatorial position. The Re(1)–Re(2)–Cl(2) bond angle of 117.3° is almost 9° wider than the largest comparable angle of 108.7(1)° in $Re_2(O_2CC_2H_5)(L^3)_2Cl_3$ (L^3 = 2-methyl-6-hydroxypyridinato).[8] Nevertheless, most bond distances and angles in **2** are similar to those in the three other examples of this type of complex.[9]

Table 4 Comparison of measured (X-ray) and calculated (DFT) molecular dimensions (Å)

	$Re_2(hpp)_4Cl_2$		$Re_2(DTolF)_4Cl_2$	
	X-ray	DFT	X-ray	DFT
Re–Re	2.191(1)	2.23	2.2759(3)	2.28
Re–Cl	2.749(5)	2.78	2.528(2)	2.59
Re–N	2.070(7)	2.16	2.099(6)	2.14

Theoretical study

In previous publications from this laboratory, it has been shown that density functional theory (DFT) can be used very successfully to reproduce the molecular structures and to elucidate the bonding in M_2^{n+} complexes where M is an element from the second transition series.[10] What we report here is the first application of DFT to an M_2^{n+} compound where M is from the third transition series.

The DFT method employed was B3LYP, Beck's three parameter hybrid exchange functional[11] and the Lee–Yang–Parr nonlocal correlation functional.[12] The basis set used was an [8s5p4d2f] contraction of the (15s10p9d3f) primitive set augmented with a p-like polarization function by Huzinaga[13] for Re and the valence double-zeta basis set augmented with d and p-like polarization functions[14] (6-31G(d,p)) for all other atoms. Analytic gradient methods were used for geometry optimization. Gaussian-94[15] was used for the computations and Cerius 2[16] was used to generate the graphic images of the molecular orbitals.

The optimized structure has idealized D_4 symmetry and the geometric parameters are in good agreement with the experimental results, as shown in Table 4. The theoretical Re–Re bond distance is 2.23 Å, about 0.04 Å longer than the experimental value (2.19 Å). The calculated Re–Cl atomic distance of 2.78 Å is 0.03 Å longer than found in the crystal structure. The Re–N bond length is calculated to be 2.16 Å, which is 0.09 Å longer than the experimental value. Although relativistic effects have not been included in the calculation, the good geometry prediction suggests that the DFT method is applicable in third row metal–metal bond studies. Current studies in our laboratory indicate that relativistic effects are not of major importance as long as a full electron basis set is used.[17]

The orbitals of predominately metal–metal bonding character are depicted on the right side of Fig. 3, in which $b_2(\delta)$ is the highest occupied molecular orbital (HOMO, 242) and the $b_1(\delta^*)$ is the lowest unoccupied molecular orbital (LUMO, 243). The energy gap between the HOMO and LUMO is 2.47 eV. The Re–Re σ bonding is shared between the two a_1 orbitals (223,238). The π bonding is carried by the e orbitals (226,227), one of which is shown. One of the e(π*) orbitals (244,245) is shown as well as the $a_2(\sigma^*)$ orbital (246). It is clear that the two σ orbitals, and the π pair of orbitals provide a good basis for strong Re–Re bonding. As expected, the δ orbital makes only a very weak contribution.

The very long Re–Cl distances imply that the axial chlorine atoms are only weakly bonded. We can see the Re–Cl σ interactions (there are no such π or δ interactions) in two of the occupied orbitals illustrated. In MO 223 there is a bonding interaction, but this is counteracted by the antibonding interaction in MO 238.

It should also be noted that both the π and δ orbitals (226, 227 and 242) show considerable interaction of the metal orbitals with the hpp ligand orbitals. This is another good illustration of the fact that the metal–metal interactions cannot, in general, be properly considered independently of their further perturbation by interactions with the ligand π orbitals.

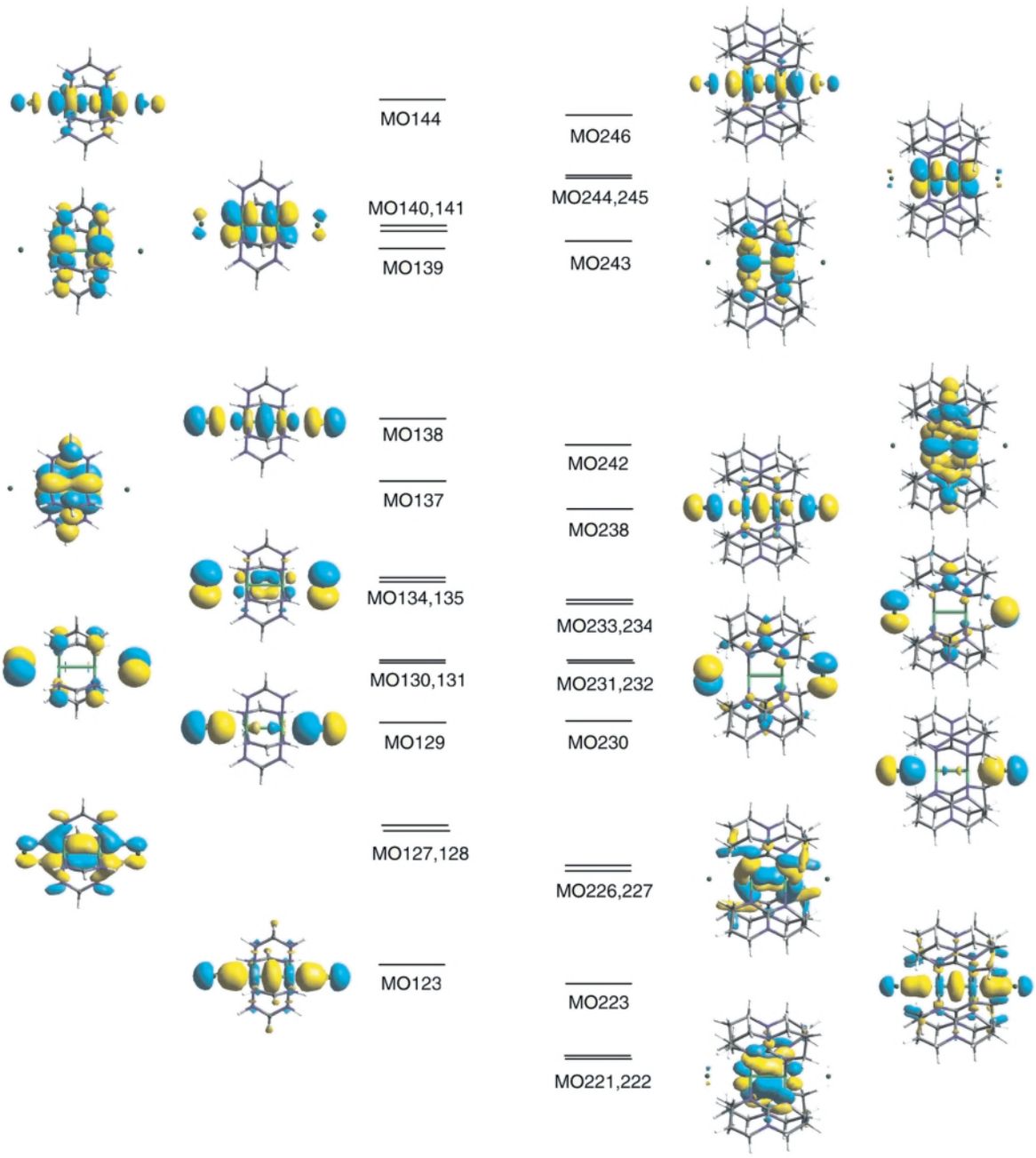

Fig. 3 The comparison of the predominantly metal–metal bonding orbitals in $Re_2(HNCHNH)_4Cl_2$ and $Re_2(hpp)_4Cl_2$. The HOMO is $a_{1g}(\sigma-\sigma(Cl))$ for $Re_2(HNCHNH)_4Cl_2$, and $b_2(\delta)$ for $Re_2(hpp)_4Cl_2$. The drawings corresponding to each electronic state are depicted in a zig-zag manner. For example, those on the far right correspond from bottom to top to MO's 223, 230, (233,234), 242 and (244,245).

In the early studies of dirhenium formamidinate complexes, the model complex $Re_2(HNCHNH)_4Cl_2$ had been calculated at the SCF-Xα level. Since our calculations for $Re_2(hpp)_4Cl_2$ were done using DFT, we decided to do similar calculations on the model molecule $Re_2(HNCHNH)_4Cl_2$. The optimized structure successfully reproduces the experimental measurements (Table 4) for $Re_2(DTolF)_4Cl_2$, the theoretical Re–Re bond distance, Re–Cl atomic distance, and Re–N bond length are 2.28, 2.59 and 2.14 Å, respectively, while the corresponding experimental values are 2.28, 2.53 and 2.10 Å. There is no significant difference found between the DFT and the SCF-Xα results (Fig. 4), except for the reversal of the energy sequence of the π* and δ* orbitals. However, since the DFT calculated energy difference between the π* and δ* is only 0.002 eV, this order change is insignificant. Thus the DFT and the SCF-Xα bonding pictures are consistent.

The contribution of the elements to the predominantly metal–metal bonding orbitals is listed in Table 5. It is worth noting that the metal atom contribution in MO129 of the $Re_2(HNCHNH)_4Cl_2$ model molecule is 14% while the corresponding orbital contribution for MO230 of $Re_2(hpp)_4Cl_2$ is only 3%. This orbital is seen to be bonding between the Re and Cl atoms and antibonding between the Re atoms. An increase of the percentage of the Re contribution to this orbital will certainly strengthen the Re–Cl bond and at the same time elongate the Re–Re bond distance. The change in the contribution of the Re atoms to this molecular orbital is consistent with the variations in Re–Re and Re–Cl bond lengths in $Re_2(HNCHNH)_4Cl_2$ and $Re_2(hpp)_4Cl_2$. The σ(metal core)–σ(Cl) interaction in $Re_2(hpp)_4Cl_2$ is much stronger than that in $Re_2(HNCHNH)_4Cl_2$. A further difference between these two complexes is highlighted in the π bonding of the Re–Re core. In $Re_2(HNCHNH)_4Cl_2$, there is a strong interaction with the pπ lone pairs of the Cl atoms, while in $Re_2(hpp)_4Cl_2$, the interaction is predominantly with the N atoms of the hpp ligands, as shown in Table 5 and Fig. 3.

Table 5 Contribution of the elements to the MO's

$Re_2(NHCHNH)_4Cl_2$				$Re_2(hpp)_4Cl_2$			
MO	%Re	%Cl	%(N,C)	MO	%Re	%Cl	%N,C
144 $a_{2u}(\sigma^*–\sigma^*(Cl))$	94	5	1	246 $a_2(\sigma^*–\sigma^*(Cl))$	93	6	1
140, 141 $e_g(\pi^*)$	94	6	0	244, 245 e (π^*)	98	1	1
139 $b_{1u}(\delta^*)$	72	0	28	243 $b_1(\delta^*)$	71	0	29
138 $a_{1g}(\sigma–\sigma(Cl))$	67	33	0	242 $b_2(\delta)$	67	0	33
137 $b_{2g}(\delta)$	82	0	18	238 $a_1(\sigma–\sigma(Cl))$	46	52	2
134, 135 $e_u(\pi–\pi(Cl))$	11	84	5	233, 234 e ($\pi(Cl)$)	0	86	14
130, 131 $e_g(\pi(Cl))$	9	77	14	231, 232 e ($\pi(Cl)$)	0	96	4
129 $a_{2u}(\sigma^* + \sigma^*(Cl))$	14	86	0	230 $a_2(\sigma^* + \sigma^*(Cl))$	3	97	0
127, 128 $e_u(\pi + \pi(Cl))$	57	24	19	226, 227 $e(\pi + \pi(N))$	45	0	55
123 $a_{1g}(\sigma + \sigma(Cl))$	70	25	5	223 $a_1(\sigma + \sigma(Cl))$	93	6	1
				221, 222 $e(\pi + \pi(N))$	60	1	39

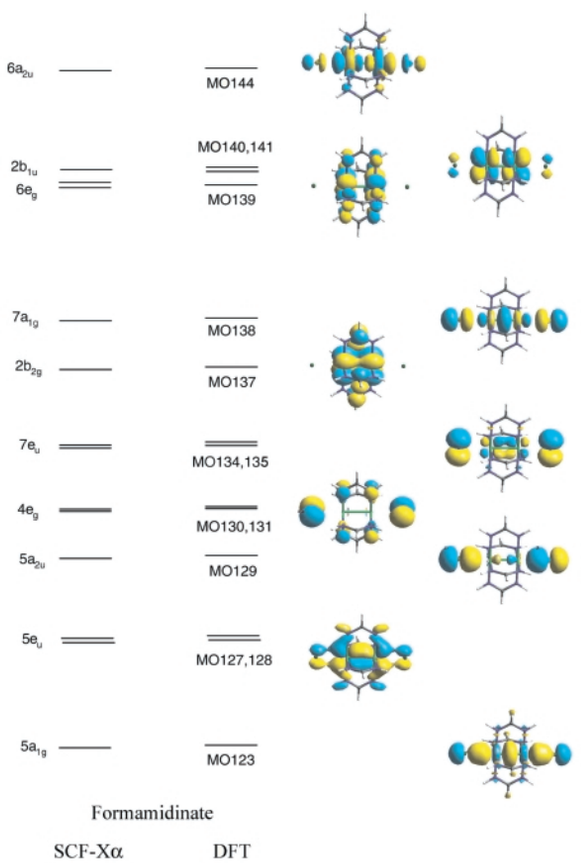

Fig. 4 The comparison of the metal–metal bonding orbitals obtained at the DFT and SCF-Xα levels for $Re_2(HNCHNH)_4Cl_2$.

Acknowledgements

We gratefully acknowledge the National Science Foundation for funding.

References

1 F. A. Cotton, *Inorg. Chem.*, 1998, **37**, 5710.
2 (*a*) F. A. Cotton, J. H. Matonic and C. A. Murillo, *J. Am. Chem. Soc.*, 1997, **119**, 7889; (*b*) F. A. Cotton, L. M. Daniels, C. A. Murillo and D. J. Timmons, *Chem. Commun.*, 1997, 1449; (*c*) F. A. Cotton, J. Gu, C. A. Murillo and D. J. Timmons, *J. Am. Chem. Soc.*, 1998, **120**, 13280; (*d*) F. A. Cotton and D. J. Timmons, *Polyhedron*, 1998, **17**, 179; (*e*) J. L. Bear, Y. Li, B. Han and K. Kadish, *Inorg. Chem.*, 1996, **35**, 1395.
3 F. A. Cotton and T. Ren, *J. Am. Chem. Soc.*, 1992, **114**, 2495.
4 F. A. Cotton and R. A. Walton, *Multiple Bonds between Metal Atoms*, Oxford University Press, 2nd edn., 1993.
5 F. A. Cotton, W. H. Ilsley and W. Kaim, *Inorg. Chem.*, 1980, **19**, 2360.
6 F. A. Cotton and L. D. Gage, *Inorg. Chem.*, 1979, **18**, 1716.
7 F. A. Cotton, L. D. Gage and C. E. Rice, *Inorg. Chem.*, 1979, **18**, 1138.
8 A. R. Cutler, S. M. V. Esjornson, P. E. Fanwick and R. A. Walton, *Inorg. Chem.*, 1988, **27**, 287.
9 F. A. Cotton, L. M. Daniels, S. C. Haefner, *Inorg. Chim. Acta*, 1999, **285**, 149.
10 F. A. Cotton and X. Feng, *J. Am. Chem. Soc.*, 1997, **119**, 7514; 1998, **120**, 3387.
11 A. D. Becke, *J. Chem. Phys.*, 1993, **98**, 5648.
12 C. Lee, W. Yang and R. G. Parr, *Phys. Rev.*, 1988, **37**, 785.
13 S. Huzinaga, *Physical Sciences Data 16: Gaussian Basis Sets for Molecular Calculations*, Elsevier, Amesterdam, Oxford, New York, Tokyo, 1984.
14 W. J. Hehre, L. Radom, P. R. Schleyer and J. A. Pople, *Ab initio Molecular Orbital Theory*, Wiley, NewYork, 1986.
15 M. J. Frisch, G. W. Trucks, H. B. Schlegel, P. M. W. Gill, B. G. Johnson, M. A. Robb, J. R. Cheeseman, T. Keith, G. A. Petersson, J. A. Montgomery, K. Raghavachari, M. A. Al-Laham, V. G. Zakrewski, J. V. Ortiz, J. B. Foresman, J. Cioslowski, B. B. Stefanov, A. Nanayakkara, M. Challacombe, C. Y. Peng, P. Y. Ayala, W. Chen, M. W. Wong, J. L. Andres, E. S. Replogle, R. Gomperts, R. L. Martin, D. J. Fox, J. S. Binkley, D. J. Defrees, J. Baker, J. P. Stewart, M. Head-Gordon, J. A. Pople, Gaussian-94, Revision D.3, Gaussian Inc., Pittsburgh, PA, 1995.
16 Cerius 2, version 3.5, Molecular Simulations Inc., 1997.
17 F. A. Cotton, J. Gu and C. A. Murillo, unpublished work.

Paper 9/04684D